Environ Geochem Health (2022) 44:2009–2020
https://doi.org/10.1007/s10653-021-00870-w

ORIGINAL PAPER

Characterization of the bioaerosol in a natural thermal cave and assessment of the risk of transmission of SARS-CoV-2 virus

Mauro Scungio · Silvia Crognale · Davide Lelli · Eleonora Carota · Giuseppe Calabrò

Received: 21 October 2020 / Accepted: 19 February 2021 / Published online: 8 March 2021

Abstract Thermal caves represent an environment characterized by unique chemical/physical properties, often used for treatment and care of musculoskeletal, respiratory, and skin diseases.

However, these environments are poorly characterized for their physical and microbiological characteristics; furthermore, the recent pandemic caused by COVID-19 has highlighted the need to investigate the potential transmission scenario of SARS-CoV-2 virus in indoor environments where an in-depth analysis of the aerosol concentrations and dimensional distributions are essential to monitor the spread of the virus.

This research work was carried out inside a natural cave located in Viterbo (Terme dei Papi, Italy) where a waterfall of sulfur–sulfate–bicarbonate–alkaline earth mineral thermal water creates a warm-humid environment with 100% humidity and 48 °C temperature. Characterization of the aerosol and bioaerosol was carried out to estimate the personal exposure to aerosol concentrations, as well as particle size distributions, and to give an indication of the native microbial load.

The data obtained showed a predominance of particles with a diameter greater than 8 μm, associated with low ability of penetration in the human respiratory system. A low microbial load was also observed, with a prevalence of noncultivable strains generated by the aerosolization of the thermal waters.

Finally, the estimation of SARS-CoV-2 infection risk by means of mathematical modeling revealed a low risk of transmission, with a decisive effect given by the mechanical ventilation system, which together with the adoption of social distancing measures makes the risk of infection extremely low.

Keywords Thermal cave · Bioaerosol · Risk of transmission · SARS-CoV-2 virus · Viral droplets · Atypical indoor environments

Supplementary information The online version contains supplementary material available at (https://doi.org/10.1007/s10653-021-00870-w)

M. Scungio · G. Calabrò
Department of Economics, Engineering, Society and Business Organization (DEIM), University of Tuscia, Via del Paradiso 47, Viterbo, Italy

S. Crognale · D. Lelli · E. Carota (✉)
Department for Innovation in Biological, Agro-Food and Forest Systems (DIBAF), University of Tuscia, Via San Camillo de Lellis, Viterbo, Italy
e-mail: carota@unitus.it

Introduction

Thermal facilities, such as caves, swimming pools, and SPAs, represent an environment characterized by unique chemical/physical properties, such as the high concentration of mineral salts and dissolved gases, peculiar temperatures and pH. Depending on the content of specific elements in the thermal waters, such as bicarbonates, calcium, sulfur, sulfates,

chlorides, radon, iron, magnesium, potassium, lithium, arsenic and silica, different therapeutic effects for musculoskeletal, respiratory, and skin diseases can be observed (Altman, 2000).

However, the recent pandemic caused by COVID-19 has imposed the need to investigate the potential transmission scenario of SARS-CoV-2 virus also in such atypical and poorly studied indoor environments, where an in-depth analysis of the aerosol concentrations and dimensional distributions are essential to monitor the spread of the virus. While some studies and models have been proposed to estimate the airborne risk of transmission in public environments such as hospitals (Chia et al., 2020; Guo et al., 2020; Liu et al., 2020) or restaurants (Buonanno et al., 2020a; Li et al., 2020), characterized by mild climatic conditions in terms of temperature and relative humidity, thermal environments have been poorly investigated; furthermore, the specific properties of these environments prevent their treatment and the application of conventional disinfection procedures in order to preserve their health benefits during balneotherapy or other treatments (Margarucci et al., 2019).

The main route of transmission of the SARS-CoV-2 virus to humans occurs predominantly via the respiratory route, by means of both small and large droplets (Morawska et al., 2020; WHO, 2020). The risk of transmission is dependent on different factors, such as droplet properties, indoor airflow, and virus characteristics. Droplet size influences both the deposition mechanisms and the extent of penetration in the human respiratory system. Small droplets (1 μm–5 μm) can remain suspended in the air for many hours and penetrate up to the alveoli, while larger droplets have a high sedimentation rate and deposit in the upper respiratory tract (Ghosh et al., 2015; Thomas et al., 2008). Moreover, being droplets constituted mostly of water associated with an aerosol-size nucleus, the evaporation kinetics, influenced by relative humidity and air temperature, affect their lifetime and deposition (Kohanski et al., 2020).

In addition to the chemical/physical characteristics of the aerosol particles, ventilation systems, and convection currents play a critical role in indoor environments: if appropriate, they can promote the removal of exhaled virus-laden air, thus lowering the airborne viral concentration; in case of inefficient or obstructed airflow, they can disperse the aerosol over a large area, with the potential to increase the risk of transmission to other occupants (Morawska et al., 2020).

The abiotic matter of the aerosol is generally associated with compounds of biological origin, including all pathogenic or nonpathogenic, live or dead fungi and bacteria, viruses, spores, pollens, and microbial secondary metabolites, which give origin to the so-called bioaerosol (Ghosh et al., 2015). Different studies concerning indoor air quality have found that between 5 and 34% of indoor air pollution is caused by biological compounds. The characterization of bioaerosol components is the subject of growing interest in the scientific community, especially for the effects that these components have on human health: infections, asthma, allergies, and other diseases of the respiratory tract (Srikanth et al., 2008).

The risks are influenced not only by the ability of the aerosol to penetrate the respiratory system, but also by its composition and biological activity. Bioaerosol composition is mainly dependent on the physical characteristics of the droplets or particles (e.g., size, density, and shape) and on environmental factors such as relative humidity, temperature, light intensity, moisture content of building material (Ghosh et al., 2015). Therefore, microbiological air quality is another important parameter to consider in a risk assessment plan.

For risk management in the initial phase of reopening of the thermal structures, some protocols and self-control plans have been developed but the development of new scientific evidence relating to this is desirable.

This research work was carried out inside a natural thermal cave located in Italy (Terme dei Papi, Viterbo) where a waterfall of sulfur–sulfate–bicarbonate–alkaline earth mineral thermal water creates a warm-humid environment with 100% humidity and 48 °C temperature. Characterization of the aerosol and bioaerosol was carried out to estimate personal exposure to aerosol concentrations in terms of number, surface area, air and mass, as well as particle size distributions, to evaluate the distribution inside the cave of these concentrations and to give an indication of the levels of the native microbial load. The final purpose was the identification of specific thresholds and alert values to support the development of a Risk Assessment Plan in thermal caves.

Materials and methods

Bioaerosol characterization

Bioaerosol active sampling

Air samples were collected by impaction with a single-stage air sampler Microflow α (AQUARIA srl, Italy), holding 380 jets with a diameter of 1 mm. The sampler was placed in a central position of the cave at 1 m height. The impaction flow rate was set at 120 L min^{-1}, and the airstream was directed on 90-mm-diameter agar Petri dishes containing different growth media, mainly Lysogeny Broth Agar (LBA) (10 g L^{-1} NaCl (Sigma-Aldrich, USA), 5 g L^{-1} yeast extract (Merck, Germany), 15 g L^{-1} agar (Difco, Michigan) and Plate Count Agar (PCA) (Difco, Michigan), or on cellulose nitrate filters with a pore size of 0.45 µm (Sartorius, Germany). Different sampling volumes, between 250 and 1000 L, were collected in duplicate. Filters were stored at −20 °C in sterile tubes until genomic DNA extraction.

Microbial load determination by cultivation-dependent technique

Petri dishes resulting from the bioaerosol active sampling were incubated for 12 h at 25 °C and 50 °C, in order to estimate the mesophilic and thermophilic microbial load, respectively. The number of microbial colonies was expressed as colony-forming units per cubic meter (CFU m^{-3}).

Quantitative PCR analysis for microbial load determination by cultivation-independent technique

Cellulose nitrate filters, deriving from bioaerosol active sampling, were used for total DNA extraction by using the DNeasy PowerWater kit (QIAGEN, Hilden, Germany) as described in the manufacturer's instructions.

Fungal and bacterial abundances were determined by q-PCR of 18S rRNA and 16S rRNA genes, respectively, on a LightCycler R 480 System (Roche Applied Science, USA). 18S rDNA sequences were amplified using the primer pair FR1F (5′-AICCATT-CAATCGGTAIT-3′) and FF 390R (5-′CGATAACGAACGAGACCT-3′), while 16S rDNA sequences using the primer pair 331F (5′-TCCTACGGGAGGCAGCAGT-3′) and 797R, (5′-GGACTACCAGGGTATCTAATCCTGTT-3′). The protocol and optimized conditions described in Crognale et al. (2019) were applied. Melting curve analysis of the PCR products was performed to confirm that the fluorescence signals were derived from specific PCR products. Fungal and bacterial concentrations were calculated based on a standard curve obtained using triplicate tenfold serial dilutions ($10^2 - 10^{10}$ 18S or 16S copy number) of known concentration of plasmid pGem T-easy cloning vector containing the target gene as the insert.

Bioaerosol passive sampling

Ninety-millimeter Petri dishes containing LBA or PCA medium were exposed to air for 2 h in a central position of the thermal cave, at 1 m height and subsequently incubated at 25 °C and 50 °C for 12 h. Counts of bacterial fungal colonies were expressed as colony-forming units per square meter per hour of exposure (CFU m^{-2} h^{-1}).

Physical characterization of aerosol

The physical characteristics of the aerosol were measured using an optical spectrometer (OPS model 3330, TSI, Minnesota, USA). The OPS was calibrated by means of tests made in the European Accredited Laboratory of Industrial Measurements (LAMI) at the University of Cassino and Southern Lazio (Italy).

The samplings were repeated in two different days and in two distinct moments: at the morning before the first entrance to the cave and at the evening after the last entrance. Each measurement represented the average of several samplings lasting 100 s and was related to a number, surface area and mass concentration and size distributions of particles per unit volume of sampled air.

Starting from the size distributions of the aerosol measured in the cave and using appropriate deposition coefficients proposed by ICRP (1994), the lung-deposited fraction of inhaled particles was calculated. In particular, the ICRP data regard different deposition coefficients which allow evaluating the fraction of inhaled aerosol particles deposited in the alveolar and tracheobronchial regions of the respiratory apparatus for different physical activities, for women and men. The deposition coefficients provided by ICRP are

specific for each particle diameter and were "fitted" to the particle size distribution considered in this study (0.3 μm–10 μm) obtaining four specific deposition curves (alveolar and tracheobronchial for woman and man considered at resting).

SARS-CoV-2 transmission risk evaluation

To evaluate the airborne transmission risk of SARS-CoV-2 inside the cave, a model recently proposed by Buonanno et al., (2020a, b) was adopted. The model is able to quantify the probability of infection due to exposure in a microenvironment in presence of a SARS-CoV-2 infected subject, utilizing a four step approach: (i) evaluation of the quanta emission rate (quanta is defined as the dose of airborne droplet nuclei required to cause infection in 63% of susceptible persons (Buonanno et al., 2020a); (ii) evaluation of the exposure to quanta concentration in the microenvironment; (iii) evaluation of the dose of quanta received by an exposed susceptible subject; and (iv) estimation of the probability of infection on the basis of a dose–response model. These four steps are briefly described, referring to the original papers for more details (Buonanno et al., 2020a, b).

The quanta emission rate (ER_q, quanta h^{-1}) is evaluated as (first step):

$$ER_q = c_v \cdot c_i \cdot IR \cdot V_d = c_v \cdot \frac{1}{C_{RNA} \cdot C_{PFU}} \cdot IR \cdot V_d$$

where c_v (RNA copies mL^{-1}) is the viral load in the exhaled droplets, c_i (quanta RNA copies $^{-1}$) is a conversion factor, IR is the inhalation rate ($m^3\ h^{-1}$), and V_d is the exhaled droplet volume concentration ($mL\ m^{-3}$), which depends on the respiratory activity.

The quanta concentration at time t to which a susceptible subject is exposed in an indoor environment is based on a mass balance and can be evaluated as (second step):

$$n\left(t, ER_q\right) = n_0 \cdot e^{-IVRR \cdot t} + \frac{ER_q \cdot I}{IVRR \cdot V} \cdot \left(1 - e^{-IVRR \cdot t}\right)$$

where IVRR (h^{-1}) represents the infectious virus removal rate, n_0 represents the initial quanta concentration, I is the number of infectious subjects, V is the volume of the indoor environment, and ER_q is the quanta emission rate for the virus under investigation. IVRR depends on three mechanisms: air exchange rate via ventilation, particle deposition on surfaces and viral inactivation. There are three important hypotheses on the quanta concentration calculation: the infectious virus removal rate is constant, the latent period of the disease is longer than the time scale of the model, and the droplets are instantaneously and evenly distributed in the indoor environment.

The dose of quanta received by an exposed susceptible subject to the quanta concentration, for a certain time interval (T), is evaluated as (third step):

$$D_q\left(ER_q\right) = IR \int_0^T n(t)dt$$

The probability of infection is calculated by an exponential dose–response model as (fourth step):

$$P_I = 1 - e^{-D_q}$$

Finally, the individual infection risk (R) of an exposed subject is calculated as the product of the probability of infection and the probability of occurrence of the specific ER_q value, while the basic reproduction number (R_0) is evaluated by multiplying the individual infection risk by the number of exposed susceptible individuals (Buonanno et al., 2020a).

Model parameters and hypothesized scenarios for the risk of infection transmission inside the cave

The parameters set as input data of the model, described in detail below, are: volume of the cave (V); total infectious viral removal rate (IVRR), which is the sum of the number of air exchanges per hour (AER), the deposition rate of particles on the surfaces (k) and rate of viral inactivation (λ), initial concentration of quanta (n_0), total time of occupation of the cave (t).

The volume of the cave was calculated directly from measurements carried out on-site and is equal to 34 m^3, while the number of hourly changes of air was obtained from the technical specifications of the ventilation system installed (260 $m^3\ h^{-1}$) plus 0.2 h^{-1} to take into account the infiltrations deriving from the partial opening of the skylight, for a total of AER equal to 7.78 h^{-1}. The deposition rate of the particles (k) was set equal to 0.24 h^{-1} as proposed by Buonanno et al. (2020a) which calculated the

deposition rate as the ratio between the sedimentation rate of particles whose diameter is greater than 1 μm (approximately 1.0×10^{-4} m s^{-1} as measured by Chatoutsidou and Lazaridis (2019) and the height of the emission source (1.5 m). The viral inactivation rate (λ) was set equal to 0.63 h^{-1} based on the value of the SARS-CoV-2 half-life (1.1 h) detected by van Doremalen et al. (2020) as follows:

$$\lambda\left(h^{-1}\right) = \frac{0.693}{t_{1/2}}$$

Finally, the initial quanta concentration (n_0) and the total occupation time of the cave (t) were set equal to zero and 8 h, respectively. All the parameters are shown in detail in Table 1.

As regards the hypothesized scenarios, these have been implemented by setting the following parameters: time of entry and exit from the cave and the emission rate of quanta of infectious subjects (ER_q); time of entry and exit from the cave and inhalation rate (IR) of the susceptible subject. In particular, we hypothesized four scenarios: the first (S1) involves the consecutive entry into the cave of two infectious subjects, for a residence time of 15 min for each, and subsequent entry into the cave of the susceptible subject, with a residence time of the latter equal to 15 min; the second (S2) involves the entry and stay of two infectious subjects and a susceptible subject simultaneously for 15 min. In the first scenario (S1), all the occupants were considered to be at rest (seated) and characterized only by respiratory activity, while in the second (S2), the occupants are considered to be standing and talking to each other. Both S1 and S2 scenarios have been implemented considering the ventilation system in operation and semi-opened skylight (AER = 7.78 h^{-1}). Starting for S1 and S2, two additional scenarios were considered: S3 (same of S1 without the ventilation system active) and S4 (same of S2 without the ventilation system active). For S3 and S4, however, an AER value of 0.2 h^{-1} was imposed to take into account infiltrations through the doors. Details of the simulated scenarios are reported in Table 2.

Results

Bioaerosol characterization inside the thermal cave

Microbiological sampling of the air is based on the capture of the corpuscular component of the aerosol, containing the biological fraction that is intended to be evaluated. The collection of airborne particles can be obtained through the use of passive sampling techniques, based on the inertial deposition of the microbiological fraction on a given surface, or through active sampling, based on the active aspiration of air with a controlled flow rate and volume of aspiration.

In Table 3, the cultivation-dependent microbial load values deriving from active and passive sampling techniques and the cultivation-independent microbial load estimated from active sampling are shown. The colonies collected in both active and passive samples were mostly bacterial (data not shown), although some rare fungal colonies were observed. Among bacteria, eight different morphotypes could be identified (Fig. S1) from both active and passive sampling, two of which presented a filamentous morphology, upon observation under an optical microscope, attributable to the group of *Actinobacteria*. Conversely, for fungi, the number of colonies isolated from both active and passive sampling was too low to be statistically representative, and although some morphotypes were identified, they were present only as a single colony. This result is also confirmed by molecular data where the value of 18S copy number m^{-3}, associated with fungal species, is two orders of magnitude lower than that of 16S, related to bacteria.

Values of microbial load deriving from passive sampling showed a predominance of thermophilic species, part of which was presumably able to grow even in mesophilic conditions. In active sampling,

Table 1 Summary of the input data used in the model for calculating the risk of infection inside the thermal cave

V (m^3)	AER (h^{-1})	k (h^{-1})	λ (h^{-1})	n_0 (quanta m^{-3})	t (min)
34	7.78	0.24	0.63	0	480

Table 2 Details of the exposure scenarios in the thermal cave implemented in the model (t_{in} time of entry into the cave, t_{out} time of exit from the cave, ER_q emission rate of quanta, IR inhalation rate, AER air exchange rate)

Scenario	Infectious subject 1			Infectious subject 2			Susceptible subject			
	t_{in} (min)	t_{out} (min)	ER_q (quanta h^{-1})	t_{in} (min)	t_{out} (min)	ER_q (quanta h^{-1})	t_{in} (min)	t_{out} (min)	IR (m^3 h^{-1})	AER (h^{-1})
S1	0	15	2.0	15	30	2.0	30	45	0.49	7.78
S2	0	15	11.4	0	15	11.4	0	15	0.54	7.78
S3	0	15	2.0	15	30	2.0	30	45	0.49	0.2
S4	0	15	11.4	0	15	11.4	0	15	0.54	0.2

Table 3 Mean concentration of the cultivation-dependent mesophilic (25 °C) and thermophilic (50 °C) microbial load, deriving from active and passive sampling, and of cultivation-independent microbial load (n° gene copy m^{-3}) from active sampling

	25 °C	50 °C	
Cultivation-dependent techniques			
Active sampling CFU m^{-3}	36 ± 5^a	28 ± 4^a	
Passive sampling CFU m^{-2} h^{-1}	3100 ± 300^b	4330 ± 240^a	
Cultivation-independent techniques			
16S copy number m^{-3}	–	–	4.99E + 04 ± 8.84E + 01
18S copy number m^{-3}	–	–	2.29E + 02 ± 3.54E−01

Different letters in apex indicate statistical significance according to Tukey's test, between values of microbial load obtained at 25 and 50 °C of incubation

instead, the mesophilic and thermophilic microbial load values are comparable, probably due to a different fraction of collected microorganisms,

Physical characteristics of the aerosol inside the thermal cave

In this section, the results of the measurements made inside the thermal cave are reported. The data are shown as size distributions (Fig. 1) and average concentrations (Table 4) in terms of the number (N), surface area (SA), and mass (M) of particles. Since no significant changes in the aerosol characteristics were observed between the two days of measurements, and between morning and evening for each day, the data are shown as average values with the relative standard deviation among all the measurements carried out.

Starting from the size distributions of the aerosol measured in the cave and using appropriate deposition curves obtained from the ICRP data for the particle size range considered in this study (0.3 – 10 μm), it is possible to estimate the fraction of particles that deposit within the respiratory system. The deposition curves are shown in Fig. 2, while a summary of the concentration in terms of the number, surface area, and mass of particles deposited in the respiratory system is reported in Table 5.

Risk of infection transmission inside the thermal cave

Based on the methodology described in "Materials and methods" section, the risk of SARS-CoV-2 transmission inside the cave is hereafter reported for the susceptible occupant (relative to his residence time) and for the susceptible persons (i.e., relative to the total time of occupation). The results of the simulations are reported in Table 6 as follows: (i) exposure time (t_{exp}) which is the occupation time in minutes for the susceptible subject and the total time of occupation for continuous occupation; (ii) individual infection risk (R) which represents the percentage probability of individual infection for the exposure to the quanta concentration profile integrated over the

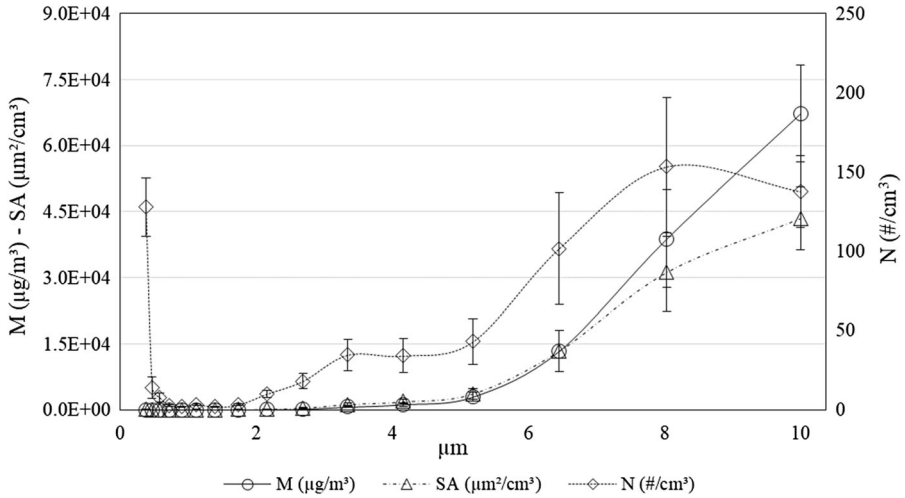

Fig. 1 Particle size distributions of the aerosol measured inside the cave in terms of mass (M, in µg m^{-3}, solid line with circles), surface area (SA, in μm^2 cm^{-3}, dashed–dotted line with triangles) and number (N, in # cm^{-3}, dotted line with diamonds) of particles per volume unit of sampled air, in the range 0.3 µm–10 µm in diameter, in 16 contiguous channels. Each dimensional channel value is reported as upper bound. The error bars represent the standard deviation in the measured data on each channel

Table 4 Average concentrations of the aerosol measured inside the cave in terms of number of particles per cm^3 of air (N), surface area of particles per cm^3 of air (SA), and mass of particles per m^3 of air (M)

	Average total concentration	Standard deviation
N (# cm^{-3})	6.9×10^2	1.3×10^2
SA (μm^2 cm^{-3})	9.5×10^4	2.2×10^4
M (µg m^{-3})	1.2×10^5	2.7×10^4

exposure time; (iii) exposure time for 1% and 0.1% risk ($t_{exp,1}$ and $t_{exp,0.1}$) which is the exposure time in minutes associated with a 1% and 0.1% probability of infection in order to consider different cohorts of individuals (younger–healthier individuals and weaker–older people, respectively); and (iv) maximum occupation of the cave for $R_0 < 1$ ($O_{max,R<1}$) which represents the maximum number of occupants theoretically allowed in the cave for the exposure time and the quanta concentration profile of the designated scenario in order to keep the base reproduction number (R_0) below 1.

In Table 6, the symbol "greater than" means that the susceptible subject or the continuous occupation does not exceed the 0.1% or 1% risk threshold.

Figure 3 shows the variation over the whole simulation time of the model results for each scenario hypothesized: quanta concentration in the cave; individual risk of infection for the susceptible subject; individual risk of infection for a subject who continuously occupies the cave for the entire simulated time; maximum theoretical occupancy of the cave to maintain $R_0 < 1$ (for a cohort that enters in the cave at the zero instant, continuous occupation).

Discussions

Bioaerosol characterization inside the thermal cave

As shown in Table 3, the active and passive sampling methods yield results that are not directly comparable, as they have different purposes: passive sampling is mainly used to measure the settling speed of particles on surfaces (CFU m^{-2} h^{-1}), while active sampling is

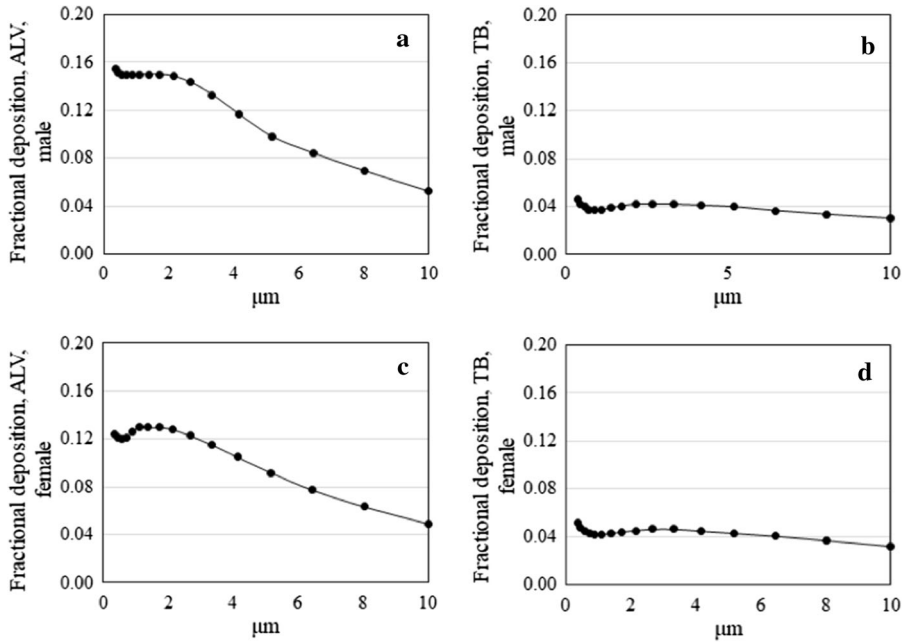

Fig. 2 Deposition curves of particles, relative to the alveolar (ALV) and tracheobronchial (TB) regions of the respiratory system specific for adult women and men at rest (seated) who breathe mainly through the nose, a typical situation of the people who occupy the thermal cave

Table 5 Particle concentration in terms of number (N), surface area (SA), and mass (M) of particles deposited in the two regions of the respiratory system per unit of volume of inhaled air inside the cave (adults at rest, male—female, ALV = alveolar region, TB = tracheobronchial region)

	Male			Female		
	ALV	TB	Total male	ALV	TB	Total female
N (# cm^{-3})	68.02	25.84	93.86	59.46	28.37	87.83
SA (μm^2 cm^{-3})	6.37×10^3	3.12×10^3	9.49×10^3	5.90×10^3	3.37×10^3	9.27×10^3
M (μg m^{-3})	7.85×10^3	4.00×10^3	1.18×10^4	7.30×10^3	4.29×10^3	1.16×10^4

Table 6 Simulation results for all the hypothesized scenarios referred to both the conditions of individual risk (susceptible subject) and continuous occupation of the thermal cave (t_{exp}: exposition time; R: individual infection risk; $t_{exp,0.1}$: exposure time for 0.1% risk; $t_{exp,1}$: exposure time for 1% risk; $O_{max,R0<1}$: maximum occupation of the cave for $R_0 < 1$, AER: air exchange ratio)

Scenario	Susceptible subject					Continuous occupation					
	t_{exp} (min)	R (%)	$t_{exp,0.1}$ (min)	$t_{exp,1}$ (min)	$O_{max,R0<1}$	t_{exp} (min)	R (%)	$t_{exp,0.1}$ (min)	$t_{exp,1}$ (min)	$O_{max,R0<1}$	AER (h^{-1})
S1	15	0.01	> 15	> 15	2742	480	0.02	> 480	> 480	605	7.78
S2	15	0.1	> 15	> 15	156	480	0.15	15	> 480	96	7.78
S3	15	0.04	> 15	> 15	386	480	0.20	54	> 480	75	0.2
S4	15	0.16	11	> 15	91	480	1.21	11	103	12	0.2

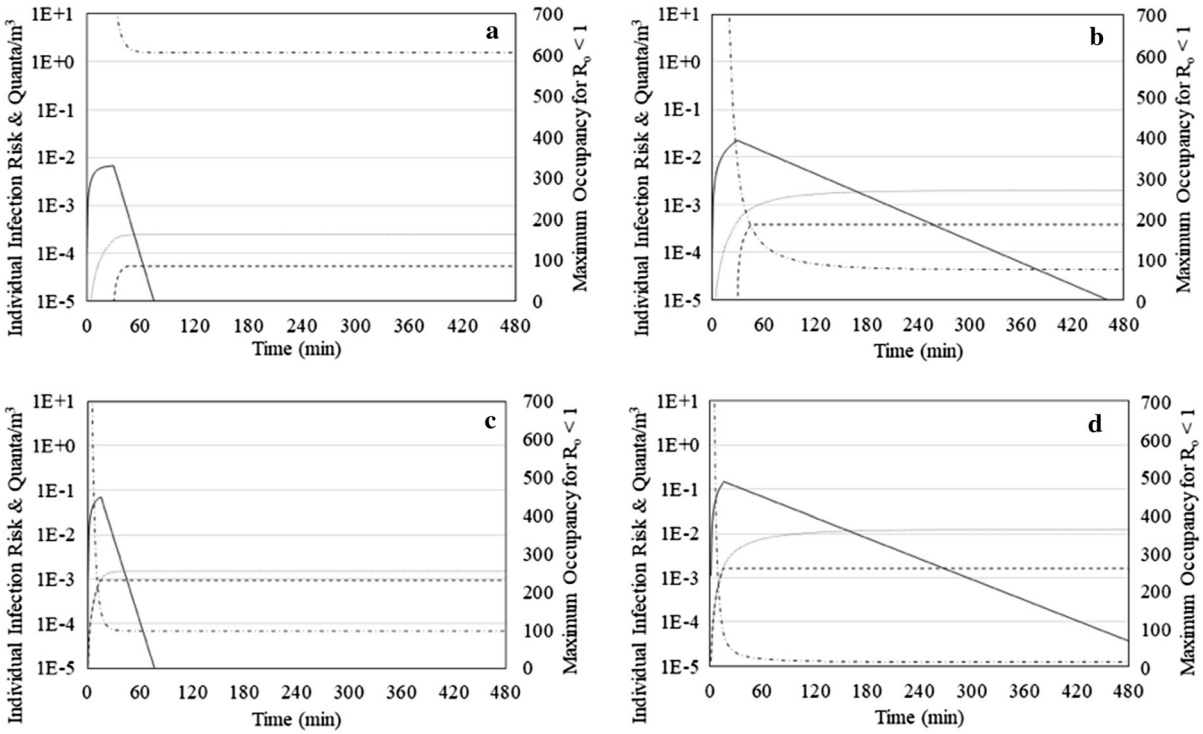

Fig. 3 Simulation results time course: scenario 1 (S1, ventilation system in operation, (**a**); scenario 2 (S2, ventilation system not in operation, (**b**); scenario 3 (S3, ventilation system in operation, (**c**) and scenario 4 (S4, ventilation system not in operation, (**d**). Quanta concentration (solid lines); continuous risk (dotted lines); individual infection risk (dashed lines) and maximum occupancy (dashed–dotted lines)

used to measure the average concentration of airborne microorganisms (CFU m^{-3}) (Cabral, 2010). Nowadays, there are no worldwide accepted regulations for microbial exposure assessment in different environments except for those elaborated for the control of the working environment summarized in four European standards: EN 13098:2000, EN 14031:2003, EN 14042:2003, and EN 14583:2004. However, these standards refer only to the methodology to be followed but do not specify threshold values for the microbial load. The only reference to evaluate the contamination levels is a document from the European Collaborative Action (EUR 14988) reporting the indicative levels of microbial air contamination by means of active sampling, the exceeding of which does not automatically imply the establishment of dangerous or unhealthy conditions.

Referring to these guidelines, a microbial load < 100 CFU m^{-3}, like that observed in the thermal cave under investigation, is considered a very low level of contamination. Given the particular conditions of the thermal environment, in addition to the reference incubation temperature for mesophilic microorganisms of 25 °C, the plates were also incubated at 50 °C to evaluate also the thermophilic microbial fraction. Even in the latter case, the microbial load values were fully within a very low level of contamination.

Regarding the passive sampling technique, although it provides an idea of the number of biological agents that undergo sedimentation per hour, it is not possible to establish any thresholds since it is not a quantitative method, it does not allow to correlate the number of microorganisms at a known volume of air and has a very low sensitivity. However, it can be considered as a qualitative parameter to describe the fate of particles in bioaerosol. In this study, the passive sampling could collect a high number of microorganisms probably because the bioaerosol was mainly composed of large-size particles (≥ 10 um) characterized by a high sedimentation rate (Cabral, 2010).

In addition to culture-dependent traditional microbiological methods, further quantification of the airborne microbial concentration was performed in this study by quantitative PCR. In fact, culture-dependent methods can only detect the viable and culturable microbial agents, leaving out a significant portion of particulates of microbial origin including viable but nonculturable and dead microorganisms; furthermore, the majority of airborne particles of microbial origin, even when viable, are nonculturable and unable to form new colonies even with appropriate media (Górny, 2020).

As expected, the amount of microbial load detected by molecular techniques was significantly higher compared to that found with methods culture-dependent, equal to one order of magnitude higher for fungi and three orders for bacteria.

Therefore, by combining molecular techniques with traditional and recognized microbiological techniques, it is possible to have a more complete picture of the microbial community present in the bioaerosol.

Physical characteristics of the aerosol inside the thermal cave

From the analysis of data relating to the physical characteristics of the aerosol measured inside the thermal cave, it can be seen that the dimensional distribution in terms of the number of particles results trimodal, with the first mode located around 0.3 μm, a second one around 3 μm and the last one around 8 μm, as shown in Fig. 1. It should be noted, anyway, that the two modes that mainly characterize the size distribution in terms of the number are the first one (0.3 μm) and the last one (8 μm), while the mode at 3 μm results less pronounced. The size distributions in terms of surface area and mass of particles, on the contrary, resulted unimodal with the mode at 10 μm (Fig. 1). From the analysis of the data, it can be stated that the dimensional distribution in number highlights the presence in the cave of a significant fraction of particles whose dimensions were below the detection threshold of the spectrometer (sub-micrometric particles) even if the fraction of particles with the mode around 8 μm were predominant. On the other hand, both the distributions in terms of surface area and mass of particles were characterized with a mode totally shifted to higher particle diameters. Summarizing, the analysis of the measured data indicated the presence in the cave of a significant fraction of sub-micrometric particles and a predominant fraction of super-micrometric particles contributing to the surface area and mass concentration. These super-micrometric particles consisted, presumably, of water droplets, while the sub-micrometric particles may consist of the solid nuclei, resulting from the evaporation of the volatile fraction, which remain suspended in the air.

Risk of infection transmission inside the thermal cave

The analysis of the data reported in Table 6 allowed to characterize the cave in terms of risk of infection under the assumptions of the model and for the considered scenarios. First of all, considering the reported data, it should be highlighted the determining effect of the mechanical ventilation system on the risk of contagion: for all the hypothesized scenarios, there is a substantial reduction in the risk of contagion considering the ventilation system active (both for the individual susceptible subject in the 15 min. of stay and for continuous occupation of the cave). This effect is made even more evident by the parameter relating to the maximum occupation of the cave (continuous occupation) which changes from the theoretical value of 75 to that of 605 (with ventilation system deactivated, S3, and activated, S1, respectively), and from 12 to 96 (with ventilation system deactivated, S4, and activated, S2, respectively). However, the purely theoretical role, albeit significant, of this parameter should be highlighted: in fact, the simultaneous presence of more occupants than the surface of an indoor environment would allow is unlikely.

Furthermore, from the analysis of the results, it is evident that the adoption of social distancing measures such as nonsimultaneous access to the cave (S1) makes the risk of contagion extremely low, according to the assumptions of the model, even with the mechanical ventilation system not active. A condition that presents a relatively high risk for the single susceptible subject is that relating to the modeled scenario with the ventilation system not active and the presence of two infectious subjects and one susceptible subject at the same time in the cave talking to each other (S4). In this case, in fact, assuming a probability of infection of 0.1%, the maximum exposure time is less than the 15-min of residence time for the susceptible subject (11 min). On the contrary, for scenario 1 with the ventilation system not active (S3),

the maximum exposure time is less than the maximum time (54 min out of 480), highlighting, once again, the fundamental role of the mechanical ventilation system. Finally, from the analysis of Fig. 3, it can be seen that the mechanical ventilation system active results in a sudden reduction in the quanta concentration in the cave (solid lines in Fig. 3) that reaches a zero value after about 75 min for both S1 and S3 scenarios and in a consequent reduction of the risk of contagion (both individual risk, dashed lines, and continuous risk, dotted lines) and increase in maximum occupancy (dashed–dotted lines). On the contrary, with the ventilation system not active, the quanta concentration reaches zero value after about 460 min for scenario 2, while for the worst hypothesized scenario (S4), the quanta concentration still remains greater than zero after the whole simulation period (480 min).

The authors want to highlight the main limitation of the model which lies in the "box model" approach, according to which the air is perfectly mixed in the cave and, consequently, the quanta concentration over time becomes uniform in space. According to this approach, susceptible individuals are therefore exposed to the same quanta concentration regardless of their position in the cave. Differences in exposure risk between susceptible occupants are therefore reduced to a function of the duration of exposure rather than their position in the cave. In light of these simplifying hypotheses, the accuracy of the model depends on the spatial scale analyzed. In general, the smaller the enclosed space, the more the air is mixed, and therefore the closer the results are to reality.

Conclusions

The microbiological characterization of the bioaerosol inside the thermal cave highlighted a low microbial load, with a prevalence of noncultivable strains generated by the aerosolization of the thermal waters. Although there are no worldwide accepted regulations for microbial air contamination, by comparing the data deriving from culture-dependent techniques with the indicative levels established by the European Collaborative Action (EUR 14988), the detected microbial load values can be classified as a very low level of contamination, therefore associated with good air quality. The physical characterization of the aerosol revealed a trimodal dimensional distribution in terms of the number of particles, with the first mode located around 0.3 μm, a second one around 3 μm and the last one around 8 μm. The size distributions in terms of surface area and mass of particles, on the contrary, resulted unimodal with the mode at 10 μm. The analysis of the measured data indicated the presence in the cave of a significant fraction of sub-micrometric particles, whose main contribution lies in the number concentration, and a predominant fraction of super-micrometric particles contributing to the surface area and mass concentration. These super-micrometric particles consisted, presumably, of water droplets, while the sub-micrometric particles may consist of the solid nuclei, resulting from the evaporation of the volatile fraction, which remain suspended in the air.

In terms of the risk of SARS-CoV-2 infection, evaluated under the hypotheses of the model, the decisive effect of the mechanical ventilation system on the risk of contagion is highlighted: for all the hypothesized scenarios, there is a substantial reduction in the risk of contagion considering the ventilation system active. Furthermore, the adoption of social distancing measures such as nonsimultaneous access to the cave makes the risk of contagion extremely low, according to the assumptions underlying the model, even with the mechanical ventilation system not active.

Acknowledgements This work has been carried out within the framework of COVID-19 activities of I-SUM/CINTEST group and has received funding from both University of Tuscia, Viterbo (Italy), under "Action for research activities related to COVID-19 emergency" Rector note n°5445, 05-05-2020 and Terme de Papi (Viterbo, Italy) within the study "Characterization of Bioaerosol in the Thermal Cave of Terme dei Papi and effect of environmental conditions in the decay and transmission of biological agents."

Authors' Contributions MS was involved in the collection, interpretation, and statistical analysis of physical data, and in the application of the mathematical model; SC helped supervise the project, conceived the experimental design, and performed the statistical analysis and interpretation of biological data. DL collected the biological samples and performed the biological experiments. EC wrote the manuscript and helped with the collection of biological samples and with the interpretation of biological results. GC secured funding for the study and supervised the project. All authors discussed the results and contributed to the final manuscript and revision.

Data availability and material Data, models, or code generated or used during the study, which are not reported in the manuscript, are available from the corresponding author by request.

Compliance with ethical standards

Conflict of interest The authors have no conflict of interest to declare that are relevant to the content of this article.

Consent to participate Consent to participate is not applicable. This article does not contain any studies involving human participants.

Consent to publish Consent to publish is not applicable. This article does not contain any studies involving human participants.

Ethical approval This article does not contain any studies involving animals or human participants performed by any of the authors. No ethical approval is required.

References

Altman, N. (2000). *Healing springs: The ultimate guide to taking the waters*. Inner Traditions/Bear & Co.

Buonanno, G., Morawska, L., & Stabile, L. (2020a). Quantitative assessment of the risk of airborne transmission of SARS-CoV-2 infection: Prospective and retrospective applications. *Environment International, 145,* 106112.

Buonanno, G., Stabile, L., & Morawska, L. (2020b). Estimation of airborne viral emission: Quanta emission rate of SARS-CoV-2 for infection risk assessment. *Environment International, 141,* 105794.

Cabral, J. P. (2010). Can we use indoor fungi as bioindicators of indoor air quality? Historical perspectives and open questions. *Science of the total environment, 408*(20), 4285–4295.

Chatoutsidou, S. E., & Lazaridis, M. (2019). Assessment of the Impact of Particulate Dry Deposition on Soiling of Indoor Cultural Heritage Objects Found in Churches and Museums/Libraries. *Journal of Cultural Heritage, 39,* 221–228.

Chia, P. Y., Coleman, K. K., Tan, Y. K., Ong, S. W. X., Gum, M., Lau, S. K., & Son, T. T. (2020). Detection of air and surface contamination by SARS-CoV-2 in hospital rooms of infected patients. *Nature Communications, 11*(1), 1–7.

Crognale, S., Stazi, S. R., Firrincieli, A., Pesciaroli, L., Fedi, S., Petruccioli, M., & D'Annibale, A. (2019). Time-dependent changes in morphostructural properties and relative abundances of contributors in *Pleurotus ostreatus/Pseudomonas alcaliphila* mixed Biofilms. *Frontiers in Microbiology, 10,* 1819.

European Collaborative Action Indoor Air Quality and its Impact on Man (formerly Cost Project 613) - Environment and Quality of Life. EUR 14988.

Ghosh, B., Lal, H., & Srivastava, A. (2015). Review of bioaerosols in indoor environment with special reference to sampling, analysis and control mechanisms. *Environment international, 85,* 254–272.

Górny, R. L. (2020). Microbial aerosols: Sources, properties, health effects, exposure assessment—a review. *KONA Powder and Particle Journal, 37,* 64–84.

Guo, Z. D., Wang, Z. Y., Zhang, S. F., Li, X., Li, L., Li, C., & Zhang, M. Y. (2020). Aerosol and surface distribution of severe acute respiratory syndrome coronavirus 2 in hospital wards, Wuhan, China, 2020. *Emerging Infectious Diseases, 26*(7), 1583–1591.

International Commission on Radiological Protection. (1994). Human respiratory tract model for radiological protection A report of a Task Group of the International Commission on Radiological Protection. *Annals of the ICRP, 24,* 1–482.

Kohanski, M. A., Lo, L. J., & Waring, M. S. (2020). Review of indoor aerosol generation, transport, and control in the context of COVID-19. *International Forum of Allergy and Rhinology, 10,* 1173–1179.

Li, Y., Qian, H., Hang, J., Chen, X., Hong, L., Liang, P., & Kang, M. (2020). Evidence for probable aerosol transmission of SARS-CoV-2 in a poorly ventilated restaurant. *medRxiv*. https://doi.org/10.1101/2020.04.16.20067728

Liu, Y., Ning, Z., Chen, Y., Guo, M., Liu, Y., Gali, N. K., et al. (2020). Aerodynamic characteristics and RNA concentration of SARS-CoV-2 aerosol in Wuhan hospitals during COVID-19 outbreak. *BioRxiv*. https://doi.org/10.1101/2020.03.08.982637

Margarucci, L. M., Romano Spica, V., Gianfranceschi, G., & Valeriani, F. (2019). Untouchability of natural spa waters: Perspectives for treatments within a personalized water safety plan. *Environment International, 133,* 105095.

Morawska, L., Tang, J. W., Bahnfleth, W., Bluyssen, P. M., Boerstra, A., Buonanno, G., & Haworth, C. (2020). How can airborne transmission of COVID-19 indoors be minimised? *Environment international, 142,* 105832.

Srikanth, P., Sudharsanam, S., & Steinberg, R. (2008). Bio-aerosols in indoor environment: Composition, health effects and analysis. *Indian journal of medical microbiology, 26*(4), 302.

Thomas, R. J., Webber, D., Sellors, W., Collinge, A., Frost, A., Stagg, A. J., et al. (2008). Characterization and deposition of respirable large-and small-particle bioaerosols. *Applied and environmental microbiology, 74*(20), 6437–6443.

Van Doremalen, N., Bushmaker, T., Morris, D. H., Holbrook, M. G., Gamble, A., Williamson, B. N., et al. (2020). Aerosol and surface stability of SARSCoV-2 as compared with SARS-CoV-1. *The New England Journal of Medicine, 382,* 1564–1567.

EN 13098:2000. (2000). Workplace Atmosphere – Guidelines for Measurement of Airborne Micro-organisms and Endotoxin.

EN 14031:2003. (2003). Workplace atmosphere-Determination of airborne endotoxins.

EN 14042: 2003. (2003). Workplace Atmospheres–Guide for the Application and Use of Procedures for the Assessment of Exposure to Chemical and Biological Agents.

EN 14583:2004. (2004). Workplace atmospheres—volumetric bioaerosol sampling devices— requirements and test methods.

World Health Organization (2020) Transmission of SARS-CoV-2: implications for infection prevention precautions: scientific brief, 09 July 2020 (No. WHO/2019-nCoV/Sci_Brief/Trasmission_modes/2020.3). World Health Organization